Optimal Performance of Constrained Control Systems

Philip S Harvey, Henri P Gavin, and Jeffrey T. Scruggs

Abstract

This paper presents a method to compute optimal open-loop trajectories for systems subject to state and control inequality constraints in which the cost function is quadratic and the state dynamics are linear. For the case in which inequality constraints are decentralized with respect to the controls, optimal Lagrange multipliers enforcing the inequality constraints may be found at any time through Pontryagin's minimum principle. In so doing, the set of differential algebraic Euler-Lagrange equations are transformed into an unconstrained nonlinear two-point boundary-value problem for states and costates whose solution meets the necessary conditions for optimality. The optimal performance of inequality constrained control systems is calculable allowing for comparison to previous, sub-optimal solutions. The method is applied to the control of damping forces in a vibration isolation system subjected to constraints imposed by the physical implementation of a particular controllable damper.

Keywords: optimal control, semi-active, dynamic programming, equipment isolation, nonlinear constraint

I. Introduction

In this paper we develop and evaluate open-loop controlled responses for systems in which each control is individually constrained. Optimal control problems involving inequality constraints are encountered in a wide range of applications [1], [2], [3], [4], [5]. In the time domain, solutions to nonlinear optimal control problems involve solving sets of Euler-Lagrange equations, i.e., differential algebraic two-point boundary value problems [6], and require iterative methods. Various methods have been proposed to find the optimal solution to inequality constrained problems. Penalty functions [7] approximately enforce constraints and require the selection of weighting constants and penalty functions. If the weighting constant is too small the constraint may not be enforced, but if it is too large, it will dominate the optimization. Sage [8] proposed introducing additional states and using Heaviside functions to convert the inequality constraint to an equality constraint. Ma and Levine [9] used a gradient descent method to iteratively converge upon the optimal controller. More recently, model predictive control or receding horizon control has become popular whereby control decisions are made online over a finite horizon [10], [11]. Johansen et al. [12] and Sznaier and Damborg [13] partition the state-space into regions where different feedback laws, calculated offline, are implemented. The latter method is only applied to free response control, i.e., in the absence of external, noncontrollable inputs, where the LQR solution is applicable. In many civil engineering applications, a sub-optimal solution is implemented in which the external input is neglected to derive the controller but then applied to the disturbed system [14]; this method is common referred to as "clipped-optimal" control and will be discussed further in this paper. Common shortcomings of the aforementioned methods are the simplicity of the constraint (i.e., linear) and/or absence of an exogenous disturbance.

Semi-active control is a class of control systems in which a small amount of external power is required to modulate mechanical properties of the actuators, i.e., stiffness [15], [16] and damping [14], [17]. Semi-active actuators are dissipative and, thus, stability constraints are not required in synthesizing controllers for

P.S. Harvey is with Department of Civil and Environmental Engineering, Duke Univ., Durham, NC 27708-0287, USA Philip.Harvey@duke.edu

H.P. Gavin is with the Faculty of Department of Civil and Environmental Engineering, Duke Univ., Durham, NC 27708-0287, USA Henri.Gavin@duke.edu

J.T. Scruggs is with the Faculty of Department of Civil and Environmental Engineering, The University of Michigan, Ann Arbor, MI 48109, USA jscruggs@umich.edu

asymptotically-stable, open-loop systems. Implementation of semi-active control involves controls acting through actuators that exhibit saturation limits [18], [19]. Therefore, the controls are sector-bounded.

Various approaches have been used in the past to synthesize control laws for semi-active vibration control problems [20]. Dating back to the early 1970's [21], [22], semi-active force generation has been studied as a means for vibration suppression for a range of applications. In particular, vehicle suspension systems [23] were of interest from the 1980's into the early 1990's. More recently semi-active control has been studied for civil engineering applications of seismic isolations of structures [18], [24], [25], [26]. This paper presents an extension of the optimal control method of Tseng and Hedrick [27] and Butsuen [28] for a more general constraint on control forces.

In this study, trajectories for optimal damping rates are calculated for vibration isolation systems that operate on the principle of a rolling pendulum. The isolated components are supported by large ball bearings (2 cm in diameter) that roll on rigid dish-shaped bowls with a quadratic profile. The period of motion is determined by the curvature of the dish, independent of the mass. Damping force is modulated in the isolation system in order to minimize a quadratic performance functional that weights total response accelerations and control efforts in order to improve the isolation system transmissibility at high frequencies while simultaneously suppressing resonant behavior. This method requires a priori knowledge of the disturbance and cannot be implemented in non-autonomous systems. However, from optimal control trajectories, parameterized feedback control laws may be deduced.

II. Methodology

This section presents the formulation and solution to optimal control problems with nonlinear decentralized constraints. The solution to the unconstrained finite-horizon linear-quadratic (LQ) problem is found by solving a two-point boundary-value problem (TPBVP) [7]. Numerical methods to solve unconstrained TPBVPs are well established, e.g., shooting methods, finite-differences, finite-elements. The method applied here is a collocation with a piecewise cubic polynomial function, which satisfies the boundary conditions for each subinterval, and is implemented by the Matlab function `bvp4c.m` [29]. This method requires an initial guess for the trajectories – states and costates – from which the nonlinear algebraic equations for the coefficients of the cubic polynomial solution are solved iteratively by linearization [30]. The contribution of this paper is to show that systems in which controls are individually constrained can be cast as an unconstrained TPBVP. In the method introduced here the constraints are enforced through Lagrange multipliers. Because controls are individually constrained, the Lagrange multipliers required to enforce constraints may be determined individually.

A. Problem Statement

An admissible control trajectory $\mathbf{u}(t) \in \mathbb{R}^m$ is to be applied to a non-autonomous system

$$\dot{\mathbf{x}} = \mathbf{f}(\mathbf{x}, \mathbf{u}, t), \qquad \mathbf{x}(0) = \mathbf{x}_0, \qquad \mathbf{x}(t) \in \mathbb{R}^n \tag{1}$$

in order to minimize a Lagrange-type cost function of the states and controls

$$J = \int_0^T L(\mathbf{x}(t), \mathbf{u}(t)) \; dt \tag{2}$$

subject to the equality constraint (1) and an ℓ-component state-control inequality constraint

$$\mathbf{c}\left(\mathbf{x}, \mathbf{u}, t\right) \leq \mathbf{0} \; . \tag{3}$$

Each constraint in $\mathbf{c}(\cdot)$ involves only one control. Hereinafter, vectors and matrices will be denoted by bold lowercase and uppercase letters, respectively. Following the calculus of variations, we define the Hamiltonian as

$$H \equiv L + \mathbf{p}^T \mathbf{f} + \boldsymbol{\lambda}^T \mathbf{c} \tag{4}$$

where $\mathbf{p}(t) \in \mathbb{R}^n$ is a Lagrange multiplier vector or costate for the dynamic constraint (1) and $\boldsymbol{\lambda}(t) \in \mathbb{R}^\ell$ are Lagrange multipliers for the inequality constraint (3). Note that all $\lambda_i(t) \geq 0$. In the usual way, adjoining the constraints with multipliers to the performance index J, we have

$$J_{\mathrm{A}} = \int_0^T H - \mathbf{p}^T \dot{\mathbf{x}} \; dt \; . \tag{5}$$

Setting the first variation of J_{A} with respect to independent increments $\delta\mathbf{x}$, $\delta\mathbf{u}$, $\delta\mathbf{p}$, and $\delta\boldsymbol{\lambda}$, i.e. $\delta J_{\mathrm{A}} = 0$, we obtain the necessary conditions for optimality. That is

$$0 = -\left.\mathbf{p}^T \delta\mathbf{x}\right|_0^T + \int_0^T \left(\frac{\partial H}{\partial \mathbf{x}} + \dot{\mathbf{p}}\right)^T \delta\mathbf{x} + \frac{\partial H}{\partial \mathbf{u}} \delta\mathbf{u} + \left(\frac{\partial H}{\partial \mathbf{p}} - \dot{\mathbf{x}}\right)^T \delta\mathbf{p} + \frac{\partial H}{\partial \boldsymbol{\lambda}}^T \delta\boldsymbol{\lambda} \; dt \; . \tag{6}$$

Note that perturbations $\delta\boldsymbol{\lambda}$ about the optimum $\boldsymbol{\lambda}^*$ are constrained: if $\boldsymbol{\lambda}^*(t) = 0$, then $\delta\boldsymbol{\lambda}(t)$ must be greater than or equal to zero, otherwise $\delta\boldsymbol{\lambda}(t)$ is unconstrained. The corresponding variation in the cost $\delta J_{\mathrm{A}}(\delta\boldsymbol{\lambda}) \leq 0$, i.e. perturbations in $\boldsymbol{\lambda}$ reduce the cost at (local) maxima. The first-order necessary conditions for optimality are thus

$$\dot{\mathbf{x}} = \frac{\partial H}{\partial \mathbf{p}} = \mathbf{f}(\mathbf{x}, \mathbf{u}, t), \qquad \mathbf{x}(0) = \mathbf{x}_0 \tag{7a}$$

$$-\dot{\mathbf{p}} = \frac{\partial H}{\partial \mathbf{x}} = \frac{\partial L}{\partial \mathbf{x}} + \frac{\partial \mathbf{f}^T}{\partial \mathbf{x}} \mathbf{p} + \frac{\partial \mathbf{c}^T}{\partial \mathbf{x}} \boldsymbol{\lambda}, \qquad \mathbf{p}(T) = \mathbf{0} \tag{7b}$$

$$\mathbf{0} = \frac{\partial H}{\partial \mathbf{u}} = \frac{\partial L}{\partial \mathbf{u}} + \frac{\partial \mathbf{f}^T}{\partial \mathbf{u}} \mathbf{p} + \frac{\partial \mathbf{c}^T}{\partial \mathbf{u}} \boldsymbol{\lambda} \tag{7c}$$

$$\mathbf{0} \geq \frac{\partial H}{\partial \boldsymbol{\lambda}} = \mathbf{c}(\mathbf{x}, \mathbf{u}, t) \; . \tag{7d}$$

Equations (7a)–(7d) constitute a constrained TPBVP which, in general, can be extremely hard to solve.

In the case of linear, time-invariant (LTI) state dynamics

$$\dot{\mathbf{x}} = \mathbf{f}(\mathbf{x}, \mathbf{u}, t) = \mathbf{A}\mathbf{x}(t) + \mathbf{B}\mathbf{u}(t) + \mathbf{G}\mathbf{w}(t), \qquad \mathbf{x}(0) = \mathbf{x}_0, \qquad \mathbf{x}(t) \in \mathbb{R}^n \tag{8}$$

where $\mathbf{w}(t)$ is an exogenous input, and the Lagrangian is quadratic

$$L(\mathbf{x}(t), \mathbf{u}(t)) = \frac{1}{2} \begin{bmatrix} \mathbf{x} \\ \mathbf{u} \end{bmatrix}^T \begin{bmatrix} \mathbf{Q} & \mathbf{S} \\ \mathbf{S}^T & \mathbf{R} \end{bmatrix} \begin{bmatrix} \mathbf{x} \\ \mathbf{u} \end{bmatrix} \tag{9}$$

the necessary conditions (7a)-(7d) reduce to

$$\dot{\mathbf{x}} = \frac{\partial H}{\partial \mathbf{p}} = \mathbf{A}\mathbf{x} + \mathbf{B}\mathbf{u} + \mathbf{G}\mathbf{w}, \qquad \mathbf{x}(0) = \mathbf{x}_0 \tag{10a}$$

$$-\dot{\mathbf{p}} = \frac{\partial H}{\partial \mathbf{x}} = \mathbf{Q}\mathbf{x} + \mathbf{S}\mathbf{u} + \mathbf{A}^T \mathbf{p} + \frac{\partial \mathbf{c}^T}{\partial \mathbf{x}} \boldsymbol{\lambda}, \qquad \mathbf{p}(T) = \mathbf{0} \tag{10b}$$

$$\mathbf{0} = \frac{\partial H}{\partial \mathbf{u}} = \mathbf{R}\mathbf{u} + \mathbf{S}^T \mathbf{x} + \mathbf{B}^T \mathbf{p} + \frac{\partial \mathbf{c}^T}{\partial \mathbf{u}} \boldsymbol{\lambda} \tag{10c}$$

$$\mathbf{0} \geq \frac{\partial H}{\partial \boldsymbol{\lambda}} = \mathbf{c}(\mathbf{x}, \mathbf{u}, t) \; . \tag{10d}$$

Henceforth, the linear quadratic (LQ) problem will be handled, but the proposed methods are viable for nonlinear dynamics and arbitrary Lagrangians.

Though these necessary conditions are well-known, methods to find solutions are not well represented for complex constraints $\mathbf{c}(\cdot)$, i.e., non-linear and/or state constraints. Here, we present a saturation method in which knowledge of the decentralized structure of the constraint boundaries allows for closed-form expressions for the optimal Lagrange multiplier values. This is an extension of Butsuen's work [28] which involved linear constraints on the a single actuator system with only state weight in the cost.

The extensions presented here allow for exogenous disturbances and multiple controls subject to a much broader class of constraints involving controls and states. By recognizing that control constraints are decentralized, i.e., each constraint equation involves only one control input, it will become evident in the following that optimal values of the constraint Lagrange multipliers may be found in closed form from $\frac{\partial H}{\partial \mathbf{u}} = \mathbf{0}$.

B. Optimal Constrained Control Law

Numerical solutions to (10a)–(10d) are represented by four trajectories—$\mathbf{u}(t)$, $\mathbf{x}(t)$, $\boldsymbol{\lambda}(t)$, and $\mathbf{p}(t)$. Controls and Lagrange multipliers that satisfy the stationarity condition (10c) and control constraints (10d) may be evaluated for each time step and inserted into the state and costate dynamics, (10a) and (10b), thereby resulting in an unconstrained TPBVP. This method involves a saturation procedure described below.

At the optimal solution, the complementary slackness condition

$$\lambda_j(t) \begin{cases} = 0, & c_j(\mathbf{x}, u_j, t) < 0 \\ \geq 0, & c_j(\mathbf{x}, u_j, t) = 0 \end{cases} \tag{11}$$

must hold, i.e., improvements can only come by violating the constraint. Pontryagin's Minimum Principle [6] states the optimal control is the one that minimizes the value of the Hamiltonian $H(\cdot)$ at any particular instant:

$$\mathbf{u}^*(t) = \arg \min_{\mathbf{u}(t)} \{H(\mathbf{x}, \mathbf{u}, \mathbf{p}, \boldsymbol{\lambda}, t)\} \tag{12}$$

or equation (10c). This minimization must respect constraint (10d), but is essentially an algebraic problem at each instant in time [31]. The difficulty arrises in computing the solution to the state/costate system of equations in the form of a TPBVP.

The optimal control $\mathbf{u}(t)$ and inequality constraint multiplier $\boldsymbol{\lambda}(t)$ are found from (10c) as follows: define the proposed control to be

$$\tilde{\mathbf{u}}(t) \equiv -\mathbf{R}^{-1}\left(\mathbf{S}^T\mathbf{x}(t) + \mathbf{B}^T\mathbf{p}(t)\right) \ . \tag{13}$$

This is the optimal unconstrained (or active) control given by (10c) where $\boldsymbol{\lambda}(t) \equiv \mathbf{0}$. Unless constraints are redundant or over-specified, no more than one constraint per control input is invoked at any point in time; we saturate the control to the most restrictive constraint. Furthermore, each constraint is assumed to be decentralized with respect to its control, i.e. $\mathbf{c}(\mathbf{x}, \mathbf{u}, t) = \left[\mathbf{c}^{(1)}(\mathbf{x}, u_1, t)^T \ \cdots \ \mathbf{c}^{(m)}(\mathbf{x}, u_m, t)^T\right]^T$ where $\mathbf{c}^{(k)}(\cdot) \in \mathbb{R}^{\ell_k}$ and $\sum_k \ell_k = \ell$. Similarly, the inequality constraint Lagrange multipliers can be partitioned as follows: $\boldsymbol{\lambda}(t) = [\boldsymbol{\lambda}^{(1)}(t)^T \ \cdots \ \boldsymbol{\lambda}^{(m)}(t)^T]^T$. This allows for determination of each optimal control $u_k(t)$ independently of the other controls. So at most, only one multiplier $\lambda_j^{(k)}(t)$ will be activated at any time for a given control $u_k(t)$. If $c_j^{(k)}(\mathbf{x}, \tilde{u}_k, t) \leq 0 \ \forall \ j$, accept $u_k(t) = \tilde{u}_k(t)$; otherwise, $\lambda_j^{(k)}(t)$ must be determined such that the violated constraint $c_j^{(k)}(\mathbf{x}, u_k, t) = 0$. To this end, we define the saturation function as follows:

$$\begin{aligned} \mathrm{Sat}(\mathbf{x}, u_k; t) \equiv &\begin{cases} u_k : & c_j^{(k)}(\mathbf{x}, u_k, t) \leq 0 \ \forall \ j \\ \hat{u}_k : & c_i^{(k)}(\mathbf{x}, u_k, t) > 0 \end{cases} \\ \text{such that} \quad & c_i^{(k)}(\mathbf{x}, \hat{u}_k, t) = 0 \ . \end{aligned} \tag{14}$$

A visualization of the saturation function is given in Figure 1. The leftmost figure, Figure 1(a), shows a feasible proposed control, i.e., $c_j^{(k)}(\mathbf{x}, u_k, t) \leq 0 \ \forall \ j$; therefore, we accept $u_k(t) = \tilde{u}_k(t)$. Next, Figure 1(b) depicts a simple saturation of an infeasible proposal constraint, $c_2^{(k)}(\mathbf{x}, \tilde{u}_k, t) > 0$; $\tilde{u}_k(t)$ is saturated to $\hat{u}_k$ such that $c_2^{(k)}(\mathbf{x}, \hat{u}_k, t) = 0$. Finally, Figure 1(c) shows a scenario where two constraints are not satisfied; in this case, we saturate to the most restrictive constraint, $c_1^{(k)}(\mathbf{x}, \hat{u}_k, t) = 0$.

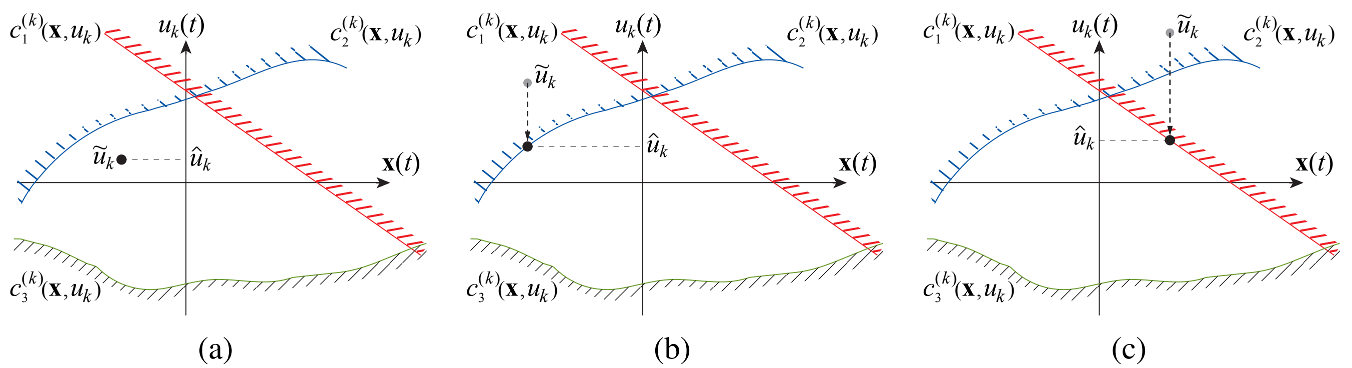

Fig. 1. Saturation function visualization in extended state space. (a) Accept $\hat{u}_k = \tilde{u}_k$; (b) saturate $\tilde{u}_k$ to nearest constraint boundary, $c_2^{(k)}(\mathbf{x}, \hat{u}_k) = 0$; and (c) saturate $\tilde{u}_i$ to most restrictive constraint, $c_1^{(k)}(\mathbf{x}, \hat{u}_k) = 0$.

Once all optimal $u_k(t)$ have been determined, it's a matter of finding the corresponding optimal $\lambda_j^{(k)}(t)$. Note that because the constraints are decentralized and each control will adhere to at most one active constraint, at most m Lagrange multipliers $\lambda_j^{(k)}(t)$ need to be determined. In the case where $\tilde{u}_k(t)$ is feasible, Lagrange multipliers $\boldsymbol{\lambda}^{(k)}(t) = \mathbf{0}$; if $\tilde{u}_k(t)$ violates constraint $c_i^{(k)}(\mathbf{x}, u_k, t)$, then Lagrange multiplier $\lambda_i^{(k)}(t)$ is found from the k^{th} equality in (10c) with all other $\lambda_l^{(k)}(t) = 0,\ l \neq i$.

The unconstrained TPBVP to be solved is now given by

$$\frac{d}{dt}\begin{bmatrix}\mathbf{x}\\ \mathbf{p}\end{bmatrix} = \begin{bmatrix}\mathbf{A} & \mathbf{0}\\ -\mathbf{Q} & -\mathbf{A}^T\end{bmatrix}\begin{bmatrix}\mathbf{x}\\ \mathbf{p}\end{bmatrix} + \begin{bmatrix}\mathbf{B}\\ -\mathbf{S}\end{bmatrix}\mathbf{u}^* + \begin{bmatrix}\mathbf{0}\\ \left.\frac{\partial \mathbf{c}^T}{\partial \mathbf{x}}\right|_{\mathbf{u}^*}\end{bmatrix}\boldsymbol{\lambda}^* + \begin{bmatrix}\mathbf{G}\\ \mathbf{0}\end{bmatrix}\mathbf{w}, \qquad \begin{bmatrix}\mathbf{x}(0)\\ \mathbf{p}(T)\end{bmatrix} = \begin{bmatrix}\mathbf{x}_0\\ \mathbf{0}\end{bmatrix} \tag{15}$$

where $\mathbf{u}^*(t) = \mathrm{Sat}(\mathbf{x}, \tilde{\mathbf{u}}; t)$ and $\boldsymbol{\lambda}^*(t)$ is the vector of corresponding optimal Lagrange multipliers. By introducing the saturation function and solving for $\boldsymbol{\lambda}^*(t)$, we have transformed the differential algebraic equation (10a)–(10d) to an unconstrained TPBVP. Note, however, that the saturation operation makes the TPBVP nonlinear.

III. A Semi-Active Isolation Model and Control Laws

To clarify and illustrate the method, open-loop controls are optimized for a vibration isolation system controlled via variable damping forces. Control trajectories are optimized to minimize peak total response accelerations when the system is excited by a pulse-like acceleration at the base. Pulse response spectra are compiled and compared to passive linear viscous damping for the single-degree-of-freedom system. Potential parameterized feedback control laws are deduced from optimal control trajectories for different excitation frequencies. Performance metrics are compared between the proposed method for a multi-degree-of-freedom isolation system, a passively-damped system, and the "clipped-optimal" feedback control [23].

Isolation systems can considerably reduce the base acceleration transmitted to objects by mechanically decoupling the object from the ground [17], [32]. Seismic equipment isolation systems are typically of two types—friction-pendulum or rolling-pendulum [33], [34], [35]—with natural periods between 2 and 4 s [32], [36]. During low-level seismic events, passive equipment isolation systems perform extremely well [37], [38], [39], [40]. Whereas, when subjected to earthquakes with high-amplitude near-fault ground motions, considerable amplification will produce excessive isolator displacements endangering the isolated object [37]. Passive damping is effective in reducing isolator drifts but at the expense of increasing equipment accelerations at high frequencies [41]. Another drawback of passive damping is the inability to adjust system parameters to achieve the desired performance objectives without a priori knowledge of the external excitation. Therefore, it would be desirable to be able to adaptively adjust system parameters in order to optimize the performance of equipment isolation systems for both near- and far- field ground

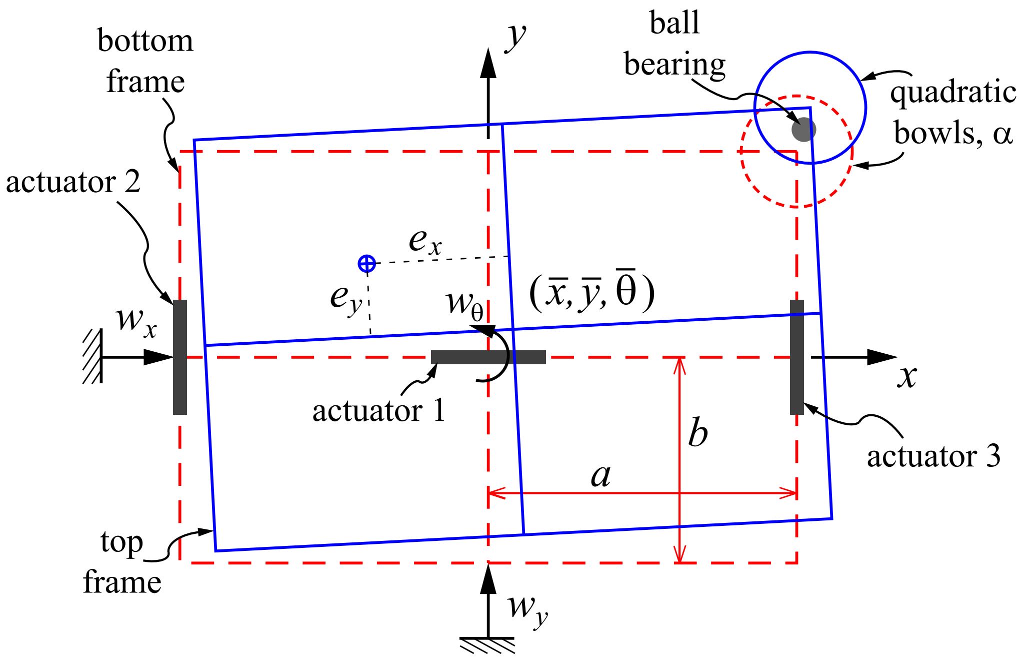

Fig. 2. Isolation platform geometry

motions. To this end, structural control, or smart isolation systems, has been proposed. In particular semi-active control systems are attractive due to their guaranteed stability and low power consumption [42], [32], [43].

A. Linear Model of an Isolation System

This section describes a LTI model of a semi-actively controlled vibration isolation system. In this study, control trajectories are found for a three-degree-of-freedom equipment isolation systems under base excitation.

Consider the semi-active isolation system shown in Figure 2 being exogenously excited by base accelerations $\ddot{w}_x$, $\ddot{w}_y$, and $\ddot{w}_\theta$. Equations of state for this system considering the kinematics of large rotations and rolling contacts [44] can be linearized in displacements $\{\bar{x}, \bar{y}, \bar{\theta}\}$, velocities $\{\dot{\bar{x}}, \dot{\bar{y}}, \dot{\bar{\theta}}\}$, and disturbance $\ddot{w}_\theta$, resulting in the following equations of motion:

$$m\left[\ddot{w}_x + \ddot{\bar{x}} - e_y(\ddot{\bar{\theta}} + \ddot{w}_\theta)\right] + F_{\mathrm{d}x} + F_{\mathrm{p}x} + F_{\mathrm{s1}} = 0 \tag{16a}$$

$$m\left[\ddot{w}_y + \ddot{\bar{y}} + e_x(\ddot{\bar{\theta}} + \ddot{w}_\theta)\right] + F_{\mathrm{d}y} + F_{\mathrm{p}y} + F_{\mathrm{s2}} + F_{\mathrm{s3}} = 0 \tag{16b}$$

$$me_x(\ddot{w}_y + \dot{\bar{y}}) - me_y(\ddot{w}_x + \dot{\bar{x}}) + \bar{I}(\ddot{w}_\theta + \ddot{\bar{\theta}}) + M_{\mathrm{d}\theta} + M_{\mathrm{dp}\theta} - aF_{\mathrm{s2}} + aF_{\mathrm{s3}} = 0 \tag{16c}$$

where

$$F_{\mathrm{d}x} \equiv 2c_{\mathrm{d}}\dot{\bar{x}}, \qquad F_{\mathrm{d}y} \equiv 2c_{\mathrm{d}}\dot{\bar{y}}, \qquad M_{\mathrm{d}\theta} \equiv 2c_{\mathrm{d}}\dot{\bar{\theta}}\left(b^2 + a^2\right)$$

$$F_{\mathrm{p}x} \equiv \frac{1}{2}mg\alpha\left(\bar{x} - e_y\bar{\theta}\right), \qquad F_{\mathrm{p}y} \equiv \frac{1}{2}mg\alpha\left(\bar{y} + e_x\bar{\theta}\right), \qquad M_{\mathrm{p}\theta} \equiv \frac{1}{2}mg\alpha\left(-e_y\bar{x} + e_x\bar{y} + a^2\bar{\theta} + b^2\bar{\theta}\right)$$

for parabolic bowls of curvature α, gravitational acceleration g of 9.81 m/s^2, and mass m of equipment resting on the top frame, taken to be 500 kg. The natural period of translational motion is given by $T_{\mathrm{n}x} = 2\pi\sqrt{2/(\alpha g)}$. In this study $\alpha = 2.0$/m and $T_{\mathrm{n}x} \approx 2$ s. Inherent damping is treated through dissipative forces acting at the ball location with damping rate c_{d}; the systems is very lightly damped ($\sim$2%).

The potential forces, $F_{\mathrm{p}x}$ and $F_{\mathrm{p}y}$, and moment, $M_{\mathrm{p}\theta}$, arrise from changes in height of the center of mass of the top frame. Dimensions of the top frame are $2a$ by $2b$ with the center of mass located at (e_x, e_y) and mass moment of inertia $\bar{I}$ about the frame's centroid, i.e., $(x, y) = (0, 0)$.

The system is actuated by semi-active forces $F_{\mathrm{s}k},\ k = 1, 2, 3$. In this application the damping force is modeled as a controllable internal force and may be interpreted as a friction coefficient acting with time lag, T_u. The response of the semi-active force may be approximated as a first order dynamic equation as follows:

$$\dot{F}_{\mathrm{s}k} = \frac{1}{T_u}\left(u_k - F_{\mathrm{s}k}\right) \tag{17}$$

where

$$u_k \equiv \text{ a target control force}$$

and T_u is between 0.02 and 0.05 second.

Equations of motion (16a–16c) may alternately be written in matrix form as follows:

$$\mathbf{M}\left(\begin{bmatrix}\ddot{\bar{x}}\\ \ddot{\bar{y}}\\ \ddot{\bar{\theta}}\end{bmatrix} + \begin{bmatrix}\ddot{w}_x\\ \ddot{w}_y\\ \ddot{w}_\theta\end{bmatrix}\right) + \mathbf{C}\begin{bmatrix}\dot{\bar{x}}\\ \dot{\bar{y}}\\ \dot{\bar{\theta}}\end{bmatrix} + \mathbf{K}\begin{bmatrix}\bar{x}\\ \bar{y}\\ \bar{\theta}\end{bmatrix} + \mathbf{F}\begin{bmatrix}F_{\mathrm{s}1}\\ F_{\mathrm{s}2}\\ F_{\mathrm{s}3}\end{bmatrix} = \mathbf{0} \tag{18}$$

where

$$\mathbf{M} \equiv \begin{bmatrix} m & 0 & -me_y\\ 0 & m & me_x\\ -me_y & me_x & \bar{I}\end{bmatrix}, \qquad \mathbf{C} \equiv \begin{bmatrix} 2c_{\mathrm{d}} & 0 & 0\\ 0 & 2c_{\mathrm{d}} & 0\\ 0 & 0 & 2c_{\mathrm{d}}(a^2+b^2)\end{bmatrix},$$

$$\mathbf{K} \equiv \frac{1}{2}mg\alpha\begin{bmatrix} 1 & 0 & -e_y\\ 0 & 1 & e_x\\ -e_y & e_x & a^2+b^2\end{bmatrix}, \qquad \mathbf{F} \equiv \begin{bmatrix} 1 & 0 & 0\\ 0 & 1 & 1\\ 0 & -a & a\end{bmatrix}.$$

By defining the state variables for this system as follows:

$$\mathbf{x} = \begin{bmatrix}\bar{x} \ \bar{y} \ \bar{\theta} \ \dot{\bar{x}} \ \dot{\bar{y}} \ \dot{\bar{\theta}} \ F_{\mathrm{s}1} \ F_{\mathrm{s}2} \ F_{\mathrm{s}3}\end{bmatrix}^T \tag{19}$$

we can rewrite equation (18) in LTI form (8) where

$$\mathbf{A} = \begin{bmatrix}\mathbf{0} & \mathbf{I} & \mathbf{0}\\ -\mathbf{M}^{-1}\mathbf{K} & -\mathbf{M}^{-1}\mathbf{C} & -\mathbf{M}^{-1}\mathbf{F}\\ \mathbf{0} & \mathbf{0} & -\frac{1}{T_u}\mathbf{I}\end{bmatrix}, \qquad \mathbf{B} = \begin{bmatrix}\mathbf{0}\\ \mathbf{0}\\ \frac{1}{T_u}\mathbf{I}\end{bmatrix}, \qquad \mathbf{G} = \begin{bmatrix}\mathbf{0}\\ -\mathbf{I}\\ \mathbf{0}\end{bmatrix}, \qquad \mathbf{w} = \begin{bmatrix}\ddot{w}_x\\ \ddot{w}_y\\ \ddot{w}_\theta\end{bmatrix}$$

and $\mathbf{I}$ is the identity matrix.

B. Semi-active force constraints

Other treatments of the semi-active vibration suppression problem [22], [23], [27] have formulated the problem as a damping rate control. In doing so, the state dynamics are bilinear in states and controls, and subsequently the costate dynamics (7b) and stationarity condition (7c) are bilinear as well [31]. The advantage of damping rate control is a simplified control constraint, i.e., $u \in [u_{\min}, u_{\max}]$. Using a force control approach simplifies the dynamics, i.e., linear state dynamics, but at the expense of a more complex (quadratic, mixed-type) state-control constraint. Unlike previous papers, we will include an additional force saturation constraint – the proposed device has a maximum damping rate as well as a peak device force [45]. In the force control framework, such a constraint is a function of the control only while in the bilinear model, such a constraint would be a mixed-type state-control constraint.

Feasible control forces are bounded by sectors shown in Figure 3. Constraining the control, u_i, consequently constrains the damping force, F_{sk}. The controllable damper has the performance limitations described by a maximum achievable damping coefficient $c_{k,\max} > 0$ and control force amplitude $u_{k,\max}$. The former limitation may be expressed by the nonlinear constraint

$$u_k \left(\frac{u_k}{c_{k,\max}} - v_k \right) \leq 0, \ \forall \ k \tag{20}$$

where v_k is the velocity across the k^{th} actuator as given by

$$\begin{aligned} v_1 &= \dot{\tilde{x}} \\ v_2 &= \dot{\tilde{y}} - a\dot{\tilde{\theta}} \\ v_3 &= \dot{\tilde{y}} + a\dot{\tilde{\theta}} \ . \end{aligned}$$

A passivity constraint is a limiting case of equation (20) whereby the damping force is merely dissipative, i.e.,

$$\lim_{c_{k,\max} \to \infty} u_k \left(\frac{u_k}{c_{k,\max}} - v_k \right) = -u_k v_k \leq 0 \tag{21}$$

In the unsaturated passive case, an arbitrarily large force u_i can be applied independent of the magnitude of the velocity. However, the device is further constrained by the force saturation limit $u_k \in [-u_{k,\max}, u_{k,\max}]$; such a constraint is given by the following inequality:

$$u_k^2 - u_{k,\max}^2 \leq 0, \ \forall \ k \ . \tag{22}$$

Thus, the quadratic state-control constraint is

$$\mathbf{c}(\mathbf{x}, \mathbf{u}; t) = \begin{bmatrix} \mathbf{c}^{(1)}(\mathbf{x}, u_1; t) \\ \mathbf{c}^{(2)}(\mathbf{x}, u_2; t) \\ \mathbf{c}^{(3)}(\mathbf{x}, u_3; t) \end{bmatrix} \leq \mathbf{0} \tag{23}$$

where

$$\mathbf{c}^{(k)}(\mathbf{x}, u_k; t) \equiv \begin{bmatrix} u_k^2 - u_{k,\max}^2 \\ \frac{u_k^2}{c_{k,\max}} - u_k v_k \end{bmatrix} \ . \tag{24}$$

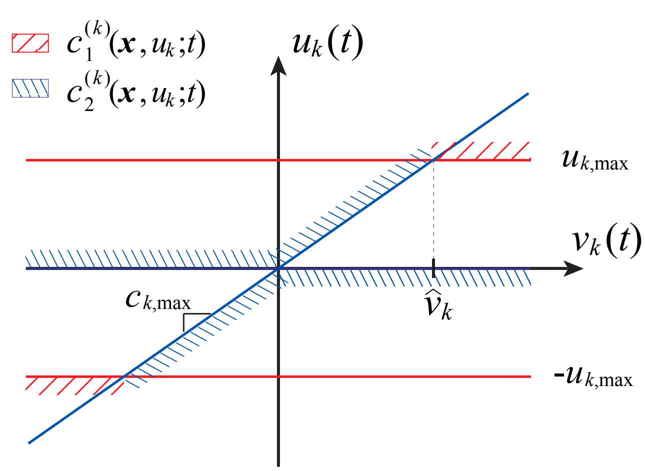

Fig. 3. Sector bound constraint for semi-active damping device.

C. Semi-active control to reduce accelerations

Consider the controlled isolation system shown in Figure 2. The equation of motion of this system is represented by an LTI form (8) with state matrices given above. In this application, the desired forces, $u_k(t)$, are sought to decrease the total acceleration experienced by the isolated mass without using too much control effort. Thus the quadratic Lagrangian $L(\cdot)$ is given by

$$L(\mathbf{x}, \mathbf{u}, t) = \frac{1}{2}\left[q_x(\ddot{x} + \ddot{w}_x)^2 + q_y(\ddot{y} + \ddot{w}_y)^2 + q_\theta(\ddot{\theta} + \ddot{w}_\theta)^2 + \rho_1 u_1^2 + \rho_2 u_2^2 + \rho_3 u_3^2\right] \ . \tag{25}$$

Letting $\mathbf{N} = [-\mathbf{M}^{-1}\mathbf{K} \ \ -\mathbf{M}^{-1}\mathbf{C} \ \ -\mathbf{M}^{-1}\mathbf{F}]$, the total accelerations are equal to $\mathbf{Nx}$ and the state weight matrix is $\mathbf{Q} = \mathbf{N}^T\text{diag}(q_x, q_y, q_\theta)\mathbf{N}$. There is no cross weight, thus, $\mathbf{S} = \mathbf{0}$. The control weight matrix is $\mathbf{R} = \text{diag}(\rho_1, \rho_2, \rho_3)$. Weights (q_x, q_y, q_θ) are chosen such that the total acceleration is dominant in the cost as opposed to the control effort; this is done because the controls constrained by (23) are inexpensive and, therefore, need not be overly-weighted.

D. Implementation of saturation function for semi-active systems

For a linear system (8) with quadratic Lagrangian (9) subject to semi-active constraints of the form given by equation (24) on each $k = 1, ..., m$ controls $u_k(t)$, the saturation function Sat$(\cdot)$ can be implemented as follows:

Define $\hat{v}_k \equiv u_{k,\max}/c_{k,max}$ to be the intersection of constraints $c_1^{(k)}(\cdot)$ and $c_2^{(k)}(\cdot)$, as shown in Figure 3, for all $k = 1, ..., m$.

1) At time t, find optimal unconstrained controls $\tilde{\mathbf{u}}(t)$ from (13).
2) For $k = 1, ..., m$, find the velocity $v_k(t)$ across k^{th} actuator and perform following test:
   a) if $|v_k(t)| \leq \hat{v}_k$, perform following checks:

$$\begin{array}{lll} i.\ \text{if } c_2^{(k)}(\mathbf{x}, \tilde{u}_k; t) \leq 0, \text{ then} & u_k^*(t) = \tilde{u}_k(t) & \\ & \lambda_1^{(k)}(t) = 0 & \lambda_2^{(k)}(t) = 0 \\ ii.\ \text{if } \tilde{u}_k(t)v_k(t) \leq 0, \text{ then} & u_k^*(t) = 0 & \\ & \lambda_1^{(k)}(t) = 0 & \lambda_2^{(k)}(t) \neq 0 \\ iii.\ \text{otherwise} & u_k^*(t) = c_{k,\max}v_k(t) & \\ & \lambda_1^{(k)}(t) = 0 & \lambda_2^{(k)}(t) \neq 0 \end{array}$$

   b) if $|v_k(t)| > \hat{v}_k$, perform following checks:

$$\begin{array}{lll} i.\ \text{if } c_1^{(k)}(\mathbf{x}, \tilde{u}_k; t) > 0, \text{ then} & u_k^*(t) = u_{k,\max}\,\text{sgn}\,(v_k(t)) & \\ & \lambda_1^{(k)}(t) \neq 0 & \lambda_2^{(k)}(t) = 0 \\ ii.\ \text{if } \tilde{u}_k(t)v_k(t) < 0, \text{ then} & u_k^*(t) = 0 & \\ & \lambda_1^{(k)}(t) = 0 & \lambda_2^{(k)}(t) \neq 0 \\ iii.\ \text{otherwise} & u_k^*(t) = \tilde{u}_k(t) & \\ & \lambda_1^{(k)}(t) = 0 & \lambda_2^{(k)}(t) = 0 \end{array}$$

   where $\text{sgn}(\cdot)$ is the signum function
3) With optimal, saturated controls $\mathbf{u}^*(t)$, solve for the corresponding optimal, non-zero $\boldsymbol{\lambda}^*(t)$ from

$$\mathbf{0} = \mathbf{R}\mathbf{u}^* + \mathbf{S}^T\mathbf{x} + \mathbf{B}^T\mathbf{p} + \left.\frac{\partial \mathbf{c}^T}{\partial \mathbf{u}}\right|_{\mathbf{u}^*} \boldsymbol{\lambda} \ .$$

The above procedure is a means of determining the optimal control and inequality constraint Lagrange multiplier instantaneously. These values are used in a numerical integration scheme such as `bvp4c.m` [29] to solve the TPBVP (15).

IV. Disturbance Model

External disturbances $\ddot{w}_x$, $\ddot{w}_y$ and $\ddot{w}_\theta$ represent an idealization of the motions of a floor of a building subjected to an earthquake ground motion. As such, it is dominated by a single frequency, $2\pi/T_p$, and grows and decays in amplitude over time. The disturbance applies inertial loads to the isolated mass, and is therefore specified in terms of an acceleration record,

$$\ddot{w}(t) = ((t-t_o)/\tau)^n \ \exp(-(t-t_o)/\tau) \ \cos(2\pi(t-t_o)/T_p - \phi) \ . \tag{26}$$

Accelerations are zero for $t < t_o$. In order for the record to contain N cycles of strong motion, the decay time constant τ is set to $NT_p/4$. If the exponent n is an integer, $\ddot{w}(t)$ can be modeled as the free response of a finite-dimensional linear system. In this study $t_{ox} = 0.25$s, $t_{oy} = t_{o\theta} = 0.5$s, $N = 2.5$ and $n = 2$. Floor acceleration records representative of structures with limited residual deformation should have negligibly small velocity and displacement at the end of the record. Integrating (26) for $n = 2$, taking the limit as $t \to \infty$, and setting this final velocity to zero leads to

$$\tan\phi = \frac{3(2\pi\tau/T_p)^2 - 1}{3(2\pi\tau/T_p) - (2\pi\tau/T_p)^3} \ . \tag{27}$$

To enforce small residual floor displacements the second derivative of a scaled logistic is iteratively subtracted from the acceleration record until the displacement at the end of the record is close to zero,

$$\ddot{w}(t) := \ddot{w}(t) - w(T) \ e^{-s}(1+e^{-s})^3(e^{-s}-1)/(\tau/2)^2 \ , \tag{28}$$

where $w(T)$ is the displacement at the end of the record (computed from $\ddot{w}(t)$ via the trapezoidal rule), and s is a scaled time variable equal to $(t - n\tau - t_o)/(\tau/2)$. This procedure for correcting for residual floor displacements converges in two or three iterations.

For $n = 2$, $N > 1$, and $0.5 < T_p < 4$ s, accelerations determined from equations (26), (27), and (28) have a peak value of about 0.54. For $n = 2$, $1 < N < 5$, and $0.5 < T_p < 4$ s, peak velocities scale with T_p and are approximately given by

$$\dot{w}_{\max} = \max\left[4.063N^{-2.165}e^{-4.403/N}, 2.329N^{-1.336}e^{-5.693/N}\right] T_p \pm 0.5\% \ . \tag{29}$$

For $N > 5$ peak velocities are approximately $0.086T_p \pm 0.5\%$. In this study disturbance waveforms were scaled to match prescribed peak velocity values, V_p, by scaling accelerations with a factor $V_p/\dot{w}_{\max}$. Figure 4 illustrates a sample of disturbance records.

The disturbance duration T is selected such that the peak response is captured without accumulating too much additional cost from transient responses. The controller we seek suppresses peak responses, and with too long of a disturbance record the optimal control may gain performance by simply damping the transient response. In all simulations duration T is found from the expression $T = 2N\max\{T_{\mathrm{p}x}, T_{\mathrm{p}y}, T_{\mathrm{p}\theta}, T_{\mathrm{n}x}\}$.

V. Simulation Results

The proposed solution method is now applied to the semi-active isolation system previously described. Values for constants are given in Table I unless otherwise stated. All three devices are assumed to be identical: $u_{i,\max} = 981$ N and $c_{i,\max} = 1566$ N-s/m, $i = 1, 2, 3$. These values correspond to 20 percent self-weight ($m = 500$ kg) and 50 percent damping in the first mode of vibration.

First, a single-degree-of-freedom system is assessed. Control trajectories are found for a range of pulse periods. At shorter period pulses ($T_{\mathrm{p}x} \in [0.4, T_{\mathrm{n}x}]$ s where $T_{\mathrm{n}x} \approx 2$ s) "pseudo-negative stiffness" [46] appears to be nearly optimal whereas, at longer period pulses ($T_{\mathrm{p}x} > T_{\mathrm{n}x}$), viscous damping is optimal. Pulse response spectra are constructed to demonstrate the performance of the optimally controlled system over a "clipped-optimal" control and two passively controlled systems with respect to four metrics: cost J, peak control forces $\max|u_1|$, peak total acceleration $\max|\ddot{\bar{x}} + \ddot{w}_x|$, and peak relative displacement $\max|\bar{x}|$.

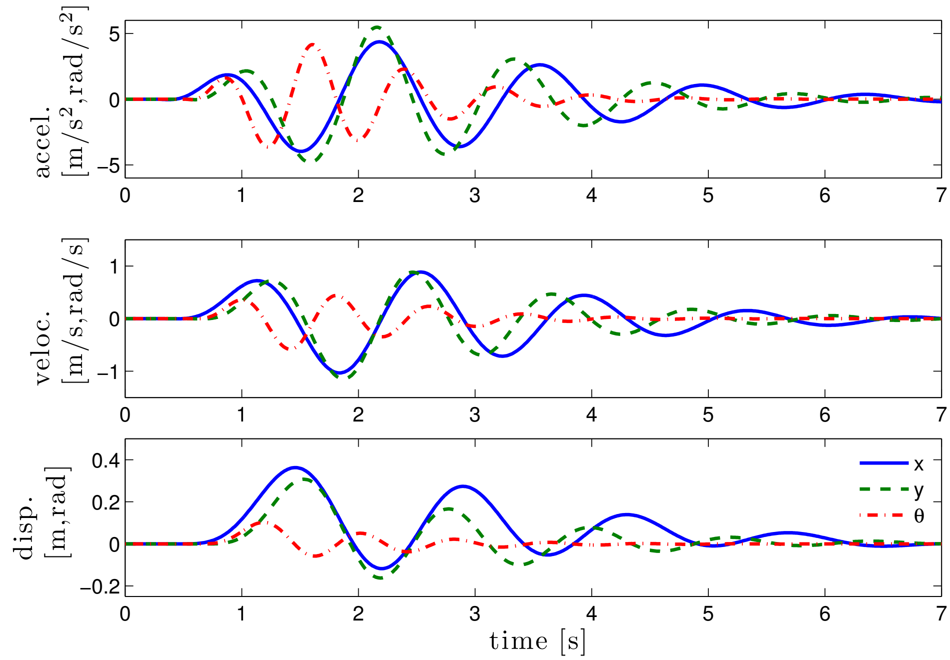

Fig. 4. Disturbance records for $V_{px} = V_{py} = 1$m/s, $V_{p\theta} = 0.5$rad/s, $T_{px} = 1.4$s, $T_{py} = 1.2$s, $T_{p\theta} = 0.8$s, $N = 2.5$, and $n = 2$. Legend: x (blue —); y (green - -); θ (red $- \cdot -$).

Next, the full three-degree-of-freedom system is analyzed. Twelve cases are investigated for a range of pulse periods and pulse velocities. Comparisons are made between trajectories found using the proposed optimal method and the "clipped-optimal" method. Performance metrics are defined and compared for the optimal method and a "clipped-optimal" scheme which are juxtaposed with a linear-visous, passively damped system as outlined in the following section.

A. Isolation Control Schemes

Here we define three control schemes, and investigate the corresponding system behaviors in Sections V-B and V-C. They are now described.

1) Scheme 1 – optimal: This uses the full dynamic optimization outlined in Section II. Finding the numerical solution of the state/costate TPBVP (15). The Matlab function `bvp4c.m` [29] is used to integrate (15).

2) Scheme 2 – clipped-optimal: This is a somewhat *ad hoc* yet prevalent sub-optimal scheme, based on linear quadratic regulator theory. In the simpler case of a linear *active* system model with quadratic cost,

TABLE I
SIMULATION PARAMETERS

bowl curvature	α	2.0	1/m
control lag	T_u	0.05	sec
ball friction damping rate	c_d	31.3	N-s/m
mass eccentricity, x	e_x	0.2	m
mass eccentricity, y	e_y	0.1	m
frame x-dimension	a	0.45	m
frame y-dimension	b	0.25	m
mass moment of inertia	$\bar{I}$	385	kg-m^2
translational state weights	q_x, q_y	m^2	
rotational state weight	q_θ	$\bar{I}^2$	
control weights	ρ_1, ρ_2, ρ_3	1.0	

the optimal control equations can reduce to a simpler problem, involving the solution of the Algebraic Riccati Equation (ARE)–see for example [23], [47]. The optimal infinite-horizon (assuming no exogenous disturbance) can be given by a simple feedback form $\mathbf{u}_{\mathrm{ARE}}(t) = \mathbf{k}\mathbf{x}(t)$ where the feedback gain vector $\mathbf{k}$ is found from solving the ARE. In order to be able to implement directly in the compliant damper model, feedback controls $\mathbf{u}_{\mathrm{ARE}}(t)$ are *clipped* when the prescribed force is infeasible.

The shortcoming of this method arises from the infinite-horizon assumption and neglecting the disturbance $\mathbf{w}(t)$. However, it does permit a feedback controller which may be implemented in real time.

3) Scheme 3 – passive: This is simple passive damper regulation. The controller is linear viscous damping, i.e., $u_i = c_{\mathrm{pass}} v_i$. Two levels of damping are considered: (a) $c_{\mathrm{pass}} = c_{\max} = 1566$ N-s/m and (b) $c_{\mathrm{pass}} = \frac{3}{5} c_{\max} = 940$ N-s/m. In both cases, the passive control force is subject to saturation limit $u_{\max} = 981$ N to make a fair comparison with the semi-active controller.

Note schemes 1 and 2 are centralized control algorithms which need the full state of the system. In the case of scheme 1, the costates are required, as well. Whereas, scheme 3 is a decentralized control algorithm which needs only the states at the actuators' locations. A decentralized control algorithm is preferable in large-scale structures where a dense sensor array becomes necessary [48]. Otherwise a nonlinear observer, e.g., classical Kalman estimator, is required to approximate the full system state. However, the goal of this project is to determine the optimal performance of a semi-active isolation system, not the most practically implementable controller.

B. Single-degree-of-freedom system

For the case in which the isolated mass has zero eccentricity and is excited uniaxially, i.e., $w_y(t) \equiv 0$ and $w_\theta(t) \equiv 0 \ \forall \ t$, the dynamics (18) decouple. If initial $\bar{y}$ displacement and $\bar{\theta}$ rotation are zero, the single-degree-of-freedom equation of motion is

$$m\ddot{\bar{x}} + 2c_{\mathrm{d}}\dot{\bar{x}} + \frac{1}{2} mg\alpha\bar{x} + F_{\mathrm{s1}} = -m\ddot{w}_x \ . \tag{30}$$

Control trajectories are found for this single-degree-of-freedom system when subjected to the pulse base excitation. Figure 5 shows the control force $u_1(t)$ versus the velocities across the actuator, $v_1(t) = \dot{\bar{x}}$. Three pulse periods are shown – 1.4, 2.0, and 2.6 seconds – which are shorter than, at, and longer than, respectively, the natural period of the system, $T_{\mathrm{n}x} \approx 2$ seconds. Also, two levels of excitation – $V_{\mathrm{p}x} = 0.5$ and 1.0 m/s, termed weak and strong, respectively – are investigated. "Pseudo-negative stiffness" [46] appears to be optimal at short pulse periods ($T_{\mathrm{p}x} < T_{\mathrm{n}x}$) when subjected to a weak excitation, whereas for a stronger excitation, the actuator is saturated, effectively squashing the "pseudo-negative stiffness" effect. At longer periods ($T_{\mathrm{p}x} > T_{\mathrm{n}x}$), linear viscous damping is optimal regardless of the input strength. Near resonance, a transition in optimality between "pseudo-negative stiffness" and linear viscous damping occurs.

Figure 6 shows four pulse-response spectra for moderate-strength excitations, $V_{\mathrm{p}x} = 1.0$ m/s. Define the ratio of the pulse period to natural period to be $\Pi_{\mathrm{p}x} \equiv T_{\mathrm{p}x}/T_{\mathrm{n}x}$. The proposed control, *scheme 1*, outperforms the three other schemes in terms of cost J, as expected; of all admissible controls satisfying (23), *scheme 1* is optimal. We note that at short-period excitations ($\Pi_{\mathrm{p}x} < 1$) the "clipped-optimal" control performs better than both the passive controls. However, beyond resonance ($\Pi_{\mathrm{p}x} > 1$) the passive controls perform better than the "clipped-optimal." Also, at long period where linear-viscous damping was seen to be optimal, the passive control with $c_{\mathrm{pass}} = c_{\max}$ performs equivalently to the optimal control.

Smaller device forces are necessary in the short-period regime ($\Pi_{\mathrm{p}x} < 0.4$); all four control schemes saturate the device for intermediate- to resonant-period excitations ($0.4 < \Pi_{\mathrm{p}x} < 1.3$; and at long-period excitations ($\Pi_{\mathrm{p}x} \geq 1.3$), the "clipped-optimal" solution requires larger device forces than both passive and optimal.

In terms of peak accelerations, the optimal and "clipped-optimal" solutions perform best at shorter pulse periods while passive and optimal perform better at longer periods. The optimal controller performs well in terms of peak acceleration because the time horizons were selected such that the peak absolute

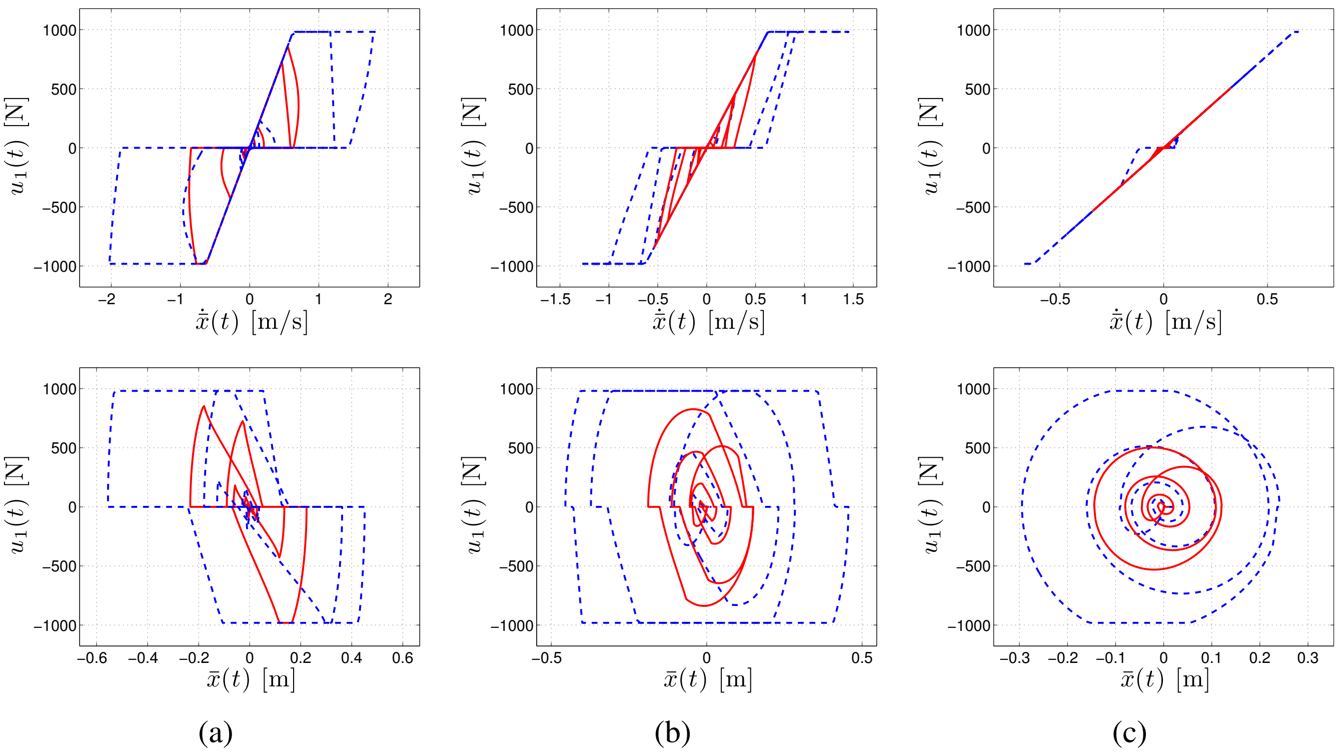

Fig. 5. Single-degree-of-freedom optimal control trajectories. Control force u_1 versus (top) velocity $\dot{\bar{x}}$ and (bottom) displacement $\bar{x}$ across actuator 1. (a) $T_{px} = 1.4$ s; (b) $T_p = 2.0$ s; (c) $T_p = 2.6$ s. Legend: (red —) $V_{px} = 0.5$ m/s; (blue - -) $V_{px} = 1.0$ m/s.

accelerations are captured but transient responses do not contribute significantly to the integral cost J. Because we use a quadratic cost, peak absolute accelerations weigh heavily on the cost.

Finally, the fourth spectrum shows the peak displacement of the isolated mass. Recall that displacement weight was not included in the cost, see Section III-C, and thus the optimal control will not necessarily perform well in terms of $\max|\bar{x}|$. In the short-period range ($\Pi_{px} < 1$), "clipped-optimal" performs relatively well but not in the long-period range ($\Pi_{px} > 1$) where the optimal control and passive control ($c_{pass} = c_{max}$) do exceedingly well.

C. *Three-degree-of-freedom system*

For the full three-degree-of-freedom isolation platform with three actuators, twelve cases are investigated for varying pulse strengths and fundamental periods by varying the disturbance parameters peak-velocities V_{px}, V_{py}, and $V_{p\theta}$ and pulse-periods T_{px}, T_{py}, and $T_{p\theta}$, respectively. The three pulse strengths investigated and the four pulse period cases are given in Table II where the natural periods of the system are $T_{nx} = 2.01$, $T_{ny} = 2.01$, and $T_{n\theta} = 0.85$ seconds.

TABLE II
SIMULATED PULSE STRENGTHS AND PERIODS

	Pulse Strength		
	V_{px} [m/s]	V_{py} [m/s]	$V_{p\theta}$ [rad/s]
Weak	0.5	0.5	0.3
Moderate	1.0	1.0	0.5
Strong	1.2	1.2	0.6

	Pulse Period		
	T_{px} [s]	T_{py} [s]	$T_{p\theta}$ [s]
Short	0.8	0.6	0.5
Intermediate	1.4	1.2	0.8
Resonant	2.4	2.2	1.0
Long	3.0	3.2	1.5

Figure 7 shows control $u_i(t)$ trajectories versus the velocity $v_i(t)$ across actuator i for four pulse period scenarios for a Moderate strength excitation. The optimal trajectory is shown along with the

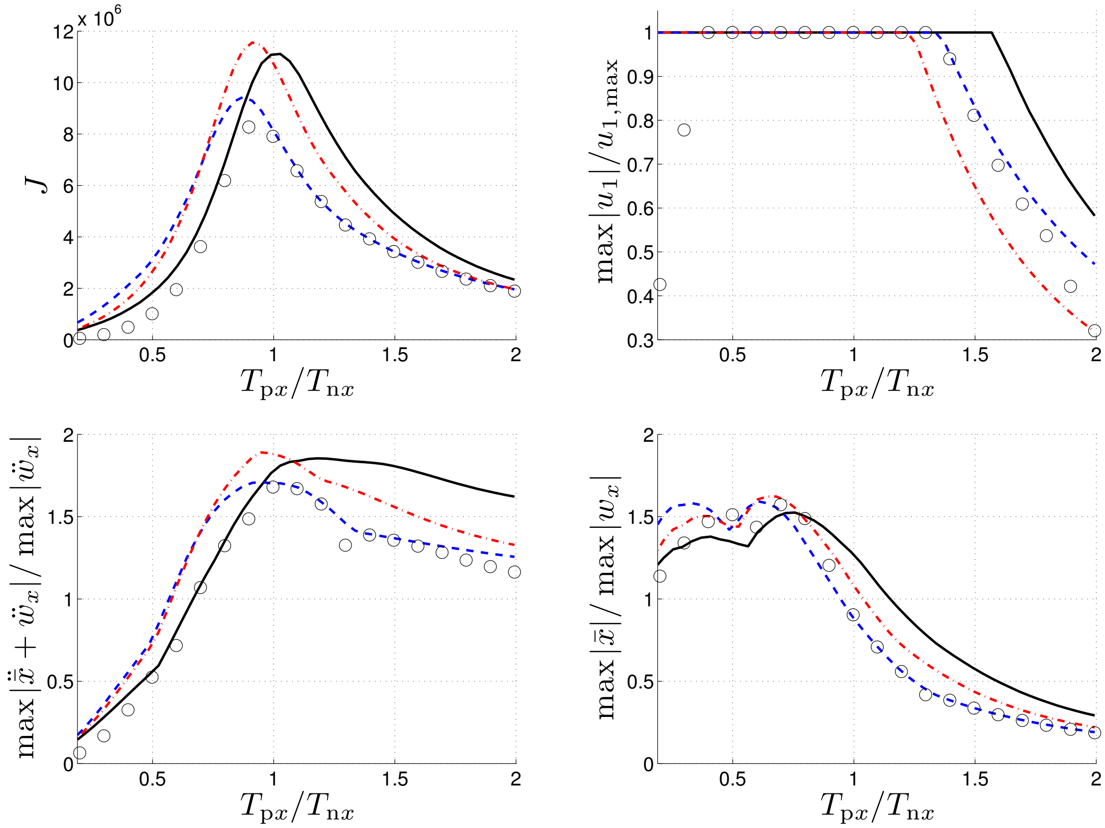

Fig. 6. Single-degree-of-freedom pulse-response spectra. Cost function, J; peak control force normalized, $\max|u_1|/u_{1,\max}$; peak total acceleration normalized, $\max|\ddot{\bar{x}}+\ddot{w}_x|/\max|\ddot{w}_x|$; and peak displacement normalized, $\max|\bar{x}|/\max|w_x|$ over a range of pulse periods T_{px}. Legend: (○) optimal; (black —) "clipped-optimal"; (blue - - -) passive $c_{\text{pass}} = 1566$ N-s/m; and (red $- \cdot -$) passive $c_{\text{pass}} = 940$ N-s/m.

"clipped-optimal" solution. These two solutions are qualitatively different especially in the longer period regimes – Resonant-period and Long-period – where the optimal control trajectory mimics linear viscous damping whereas the "clipped-optimal" solution does not. Also, velocities $v_i(t)$ are seen to be larger in the "clipped-optimal" scheme. For shorter period excitations – Short-period and Intermediate-period – controlled trajectories are more similar to one another; both controls reside within the feasible domain, not only on the boundary.

The five additional performance metrics are defined as follows:

$$\Pi_1 \equiv \frac{\max_{t,k}|u_k(t)|}{\max_k u_{k,\max}} \qquad \text{peak control force normalized} \tag{31a}$$

$$\Pi_2 \equiv \frac{\max_t|\mathbf{a}_{\text{abs}}(t)|}{\max_t|\ddot{\mathbf{w}}_r(t)|} \qquad \text{peak absolute translational acceleration normalized} \tag{31b}$$

$$\Pi_3 \equiv \frac{\max_t\left|\ddot{\bar{\theta}}(t)+\ddot{w}_\theta(t)\right|}{\max_t|\ddot{w}_\theta(t)|} \qquad \text{peak absolute rotational acceleration normalized} \tag{31c}$$

$$\Pi_4 \equiv \frac{\max_t|\mathbf{r}(t)|}{\max_t|\mathbf{w}_r(t)|} \qquad \text{peak relative radial displacement normalized} \tag{31d}$$

$$\Pi_5 \equiv \frac{\max_t\left|\bar{\theta}(t)\right|}{\max_t|w_\theta(t)|} \qquad \text{peak relative rotation normalized} \tag{31e}$$

where $\mathbf{r}(t) \equiv [\bar{x}\ \bar{y}]^T$ is the relative translation of the top frame, $\mathbf{w}_r \equiv [w_x\ w_y]^T$ is the translational base displacement vector, and $\mathbf{a}_{\text{abs}}(t) \equiv \ddot{\mathbf{r}} + \ddot{\mathbf{w}}_r$ is the absolute translational acceleration vector. These five metrics along with the cost J are compared in Table III for four control schemes: (1) optimal, (2) "clipped-optimal", and the two aforementioned clipped-passive damping schemes (3a) $c_{\mathrm{pass}} = 1566$ N-s/m and (3b) $c_{\mathrm{pass}} = 940$ N-s/m. From the table, the following conclusions could be drawn:

- At short period excitations, the optimal controller drastically outperforms linear-viscous passive systems in terms of J and peak accelerations, Π_2 and Π_3. "Clipped-optimal" also does well at short periods, with performance metrics 50% to 80% larger than optimal control.
- At longer period excitations, the optimal controller performs approximately equivalent to a linear-viscous passive device with the same maximum damping rate, $c_{\mathrm{pass}} = c_{\mathrm{max}}$. This is due to linear-viscous damping being nearly optimal in the long-period regime. "Clipped-optimal" responses are notably larger than passive responses in these cases.
- In almost all cases, "clipped-optimal" uses larger device forces than the optimal solution as well as the two passive schemes. This means that implementing the "clipped-optimal" control in practice may require larger devices to achieve equivalent performance as a passive damper, especially in the long-pulse regime.

VI. Conclusions

In this paper, a general approach to inequality constrained optimal control problems is presented. The method determines controls and Lagrange multipliers to enforce inequality state and/or control constraints while satisfying the stationarity condition. Inserting these controls and Lagrange multipliers into the state and costate equations results in an unconstrained TPBVP.

An easily implementable saturation procedure is described for a semi-active device with damping-rate and force-saturation constraints. Applying this method, the optimal performance of a semi-actively constrained isolation system is determined. Two cases were investigated: single-degree-of-freedom isolator with one actuator and the full three-degree-of-freedom system actuated by three devices. In both cases, the control force experiences a time lag arising from the modeled devices, thus raising the order of the system.

Comparisons are made between the responses of the optimal, "clipped-optimal," and viscous controlled isolation system. The results show that the responses of the optimal controller are 50% to 60% of those of the "clipped-optimal" controlled system in the short period regime, and better than those of the viscous controlled system. In the long-period range, the optimal solution is comparable to the passive viscous scheme and substantially outperforms the "clipped-optimal" controlled system.

Semi-active control systems offer the promise of far-better performance than achievable using "clipped-optimal" feedback control rules. Future work may be guided in the direction of nonlinear feedback control.

References

[1] A. Bemporad, M. Morari, V. Dua, and E. N. Pistikopoulos, "The explicit linear quadratic regulator for constrained systems," *Automatica*, vol. 38(1), pp. 3–20, 2002.

[2] P. Dua, V. Dua, and E. N. Pistikopoulos, "Optimal delivery of chemotherapeutic agents in cancer," *Computers and Chemical Engineering*, vol. 32, pp. 99–107, 2008.

[3] P. Cortés, M. P. Kazmierkowski, R. M. Kennel, D. E. Quevedo, and J. Rodríguez, "Predictive control in power electronics and drives," *IEEE Transactions on Industrial Electronics*, vol. 55(12), pp. 4312–4324, 2008.

[4] A. Bemporad and M. Morari, "Control of systems integrating logic, dynamics, and constraints," *Automatica*, vol. 35, pp. 207–427, 1999.

[5] B. Bojkov and R. Luus, "Optimal control of nonlinear systems with unspecified final times," *Chemical Engineering Science*, vol. 51(6), pp. 905–919, 1996.

[6] A. E. Bryson and Y. C. Ho, *Applied optimal control: Optimization, estimation, and control*. Washington, D.C.: Hemisphere, 1975.

[7] R. F. Stengel, *Optimal control and estimation*. New York, NY: Dover, 1994.

[8] A. P. Sage and C. C. White, *Optimum systems control*. Englewood Cliffs, NJ: Prentice-Hall, 1977.

[9] B. Ma and W. S. Levine, "An algorithm for solving control constrained optimal control problems," in *Proceedings of the 32nd IEEE Conference on Decision and Control*, 1993, pp. 3784–3790.

[10] D. Q. Mayne, J. B. Rawlings, C. V. Rao, and P. O. M. Scokaert, "Constrained model predictive control: stability and optimality," *Automatica*, vol. 36, pp. 789–814, 2000.

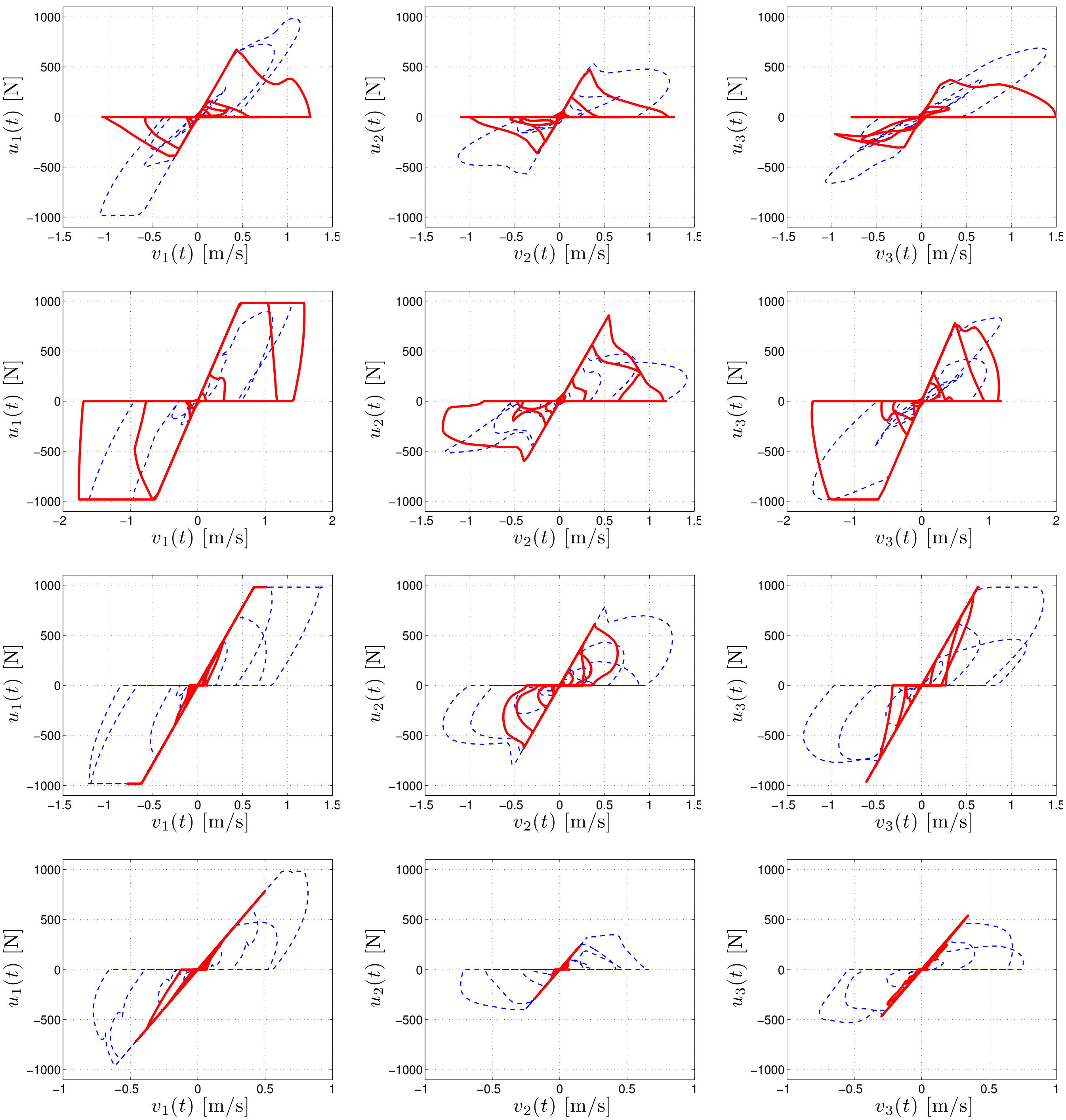

Fig. 7. Three-degree-of-freedom control $u_i(t)$ versus velocity $v_i(t)$ for Moderate strength excitation: (1st row) Short-period, (2nd row) Intermediate-period, (3rd row) Resonant-period, and (4th row) Long-period. Legend: (red —) *scheme 1*, optimal; (blue $- \cdot -$) *scheme 2*, "clipped-optimal."

[11] D. Q. Mayne and H. Michalska, "Receding horizon control of nonlinear systems," *IEEE Transactions on Automatic Control*, vol. 35(7), pp. 814–824, 1990.

[12] T. A. Johansen, I. Peterson, and O. Slupphaug, "Explicit sub-optimal linear quadratic regulation with state and input constraints," *Automatica*, vol. 38, pp. 1099–1111, 2002.

[13] M. Sznaier and M. J. Damborg, "Suboptimal control of linear systems with state and control inequality constraints," in *Proceedings of the 26th IEEE Conference on Decision and Control*, 1987, pp. 761–762.

[14] F. Sadek and B. Mohraz, "Semiactive control algorithms for structures with variable dampers," *Journal of Engineering Mechanics*, vol. 124(9), pp. 981–990, 1998.

[15] D. Nemir, Y. Lin, and R. Osegueda, "Semiactive motion control using variable stiffness," *Journal of Structural Engineering*, vol. 120(4), pp. 1291–1306, 1994.

[16] G. Leitmann, "Semiactive control for vibration attenuation," *Jorunal of Intelligent Material Systems and Structures*, vol. 5, pp. 841–846, 1994.

[17] C. Alhan, H. P. Gavin, and U. Aldemir, "Optimal control: Basis for performance comparison of passive and semiactive isolation systems," *Journal of Engineering Mechanics*, vol. 132(7), pp. 705–713, 2006.

[18] M. D. Symans and M. C. Constantinou, "Semi-active control systems for seismic protection of structures: a state- of-the-art review," *Engineering Structures*, vol. 21, pp. 469–487, 1999.

[19] S. J. Dyke, B. F. Spencer, Jr., M. K. Sain, and J. D. Carlson, "Modeling and control of magnetorheological dampers for seismic response reduction," *Journal of Smart Materials and Structures*, vol. 5, pp. 565–575, 1996.

[20] L. M. Jansen and S. J. Dyke, "Semiactive control strategies for mr dampers: Comparative study," *Journal of Engineering Mechanics*, vol. 126(8), pp. 795–803, 2000.

[21] E. Sevin and W. D. Pilkey, "Optimum shock and vibration isolations," Shock and Vibration Infomation Center, Naval Research Center, Washington, D.C., 20390, Shock and Vibration Monogram #6, 1971.

[22] D. Karnop, M. J. Crosby, and R. A. Harwood, "Vibration control using semi-active force generators," *ASME Journal of Engineering for Industry*, vol. 96, pp. 619–626, 1974.

[23] K. Yi and K. Hedrick, "Dynamics tire force control by semiactive suspension," *Journal of Dynamic Systems, Measurement, and Control*, vol. 115, pp. 465–474, 1993.

[24] D. J. Dowdell and S. Cherry, "Semi-active friction dampers for seismic response control of structures," in *Proceeding of the 5th U.S. National Conference of Earthquake Engineering*, vol. 1, Chicago, IL, 1994, pp. 819–828.

[25] H. P. Gavin and U. Aldemir, "Optimal control of earthquake response using semiactive isolation," *Journal of Engineering Mechanics*, vol. 131(8), pp. 769–776, 2005.

[26] J. T. Scruggs and W. D. Iwan, "Control of a civil structure using and electric machine with semiactive capability," *Journal of Structural Engineering*, vol. 129(7), pp. 951–959, 2003.

[27] H. E. Tseng and J. K. Hedrick, "Semi-active control laws optimal and sub-optimal," *Vehicle System Dynamics*, vol. 23, pp. 545–569, 1994.

[28] T. Butsuen, "The design of semi-active suspension for automotive vehicles," Ph.D. Thesis, Massachusetts Institute of Technology, 1989, department of Mechanical Engineering.

[29] J. Kierzenka and L. F. Shampine, "A bvp solver based on residual control and the matlab pse," *ACM Transactions on Mathematical Software*, vol. 27(3), pp. 299–316, 2001.

[30] L. F. Shampine, I. Gladwell, and S. Thompson, *Solving ODEs with Matlab*. Cambridge University Press, 2003.

[31] T. J. Gordon, "Non-linear optimal control of a semi-active vehicle suspension system," *Chaos, Solitons, & Fractals*, vol. 5(9), pp. 1603–1617, 1995.

[32] L. Y. Lu and G. L. Lin, "A theoretical study on piezoelectric smart isolation system for seismic protection of equipment in near-fault areas," *Journal of Intelligent Material Systems and Structures*, vol. 20, pp. 217–232, 2009.

[33] A. Kasalanati, A. Reinhorn, M. Constantinou, and D. Sanders, "Experimental study of ball-in-cone isolationsystem," in *Building to Last: Proceedings of the 15th Structures Congress*. New York: ASCE, 1997, pp. 1191–1195.

[34] Z. A. Kemeney, "The ball-in-cone rolling isolation system," U.S. Patent 5 599 106, February 4, 1997.

[35] B. Myslimaj, S. Gamble, D. Chin-Quee, A. Davies, and B. Breukelman, "Base isolation technologies for seismic protection of museum artifacts," in *The 2003 IAMFA Annual Conference in San Francisco, California*. San Francisco, CA: IAMFA, September 21–24 2003.

[36] F. Naeim and J. M. Kelly, *Design of Seismic Isolated Structures*. New York, NY: John Wiley & Sons, 1999.

[37] H. P. Gavin and C. Alhan, "Guidelines for low-transmissibility semi-active vibration isolation," *Journal of Smart Materials and Structures*, vol. 14, pp. 297–306, 2005.

[38] W. D. Iwan, "The earthquake design and analysis of equipment isolation systems," *Earthquake Engineering and Structural Dynamics*, vol. 6(12), pp. 523–534, 1978.

[39] Y. L. Xu, H. J. Liu, and Z. C. Yang, "Hybrid platform for vibration control of high-tech equipment in buildings subject to ground motion. part 1: Experiment," *Earthquake Engineering and Structural Dynamics*, vol. 32, pp. 1185–1200, 2003.

[40] Y. L. Xu and B. Li, "Hybrid platform for high-tech equipment protection against earthquake and microvibration," *Earthquake Engineering and Structural Dynamics*, vol. 35, pp. 943–967, 2006.

[41] J. M. Kelly, "The role of damping in seismic isolation," *Earthquake Engineering and Structural Dynamics*, vol. 28, pp. 3–20, 1999.

[42] H. P. Gavin and A. Zaicenco, "Performance and reliability of semi-active equipment isolation," *Journal of Sound and Vibration*, vol. 306, pp. 74–90, 2007.

[43] S. Nagarajaiah and S. Narasimhan, "Smart base isolated benchmark building part ii: Phase i sample controllers for linear isolation system," *Journal of Structural Control and Health Monitoring*, vol. 13(23), pp. 589–604, 2006.

[44] P. S. Harvey and H. P. Gavin, "The non-holonomic and chaotic nature of a rolling isolation system," *Nonlinear Dynamics*, 2011, (in review).

[45] C. Poussot-Vassal, O. Sename, L. Dugard, P. Gáspár, Z. Szabó, and J. Bokor, "A new semi-active suspension control strategy through lpv technique," *Control Engineering Practice*, vol. 16, pp. 1519–1534, 2008.

[46] H. Iemura and M. H. Pradono, "Simple algorithm for semi-active seismic response control of cable-stayed bridges," *Earthquake Engineering and Structural Dynamics*, vol. 34, pp. 409–423, 2005.

[47] D. Hrovat, F. Barak, and M. Rabins, "Semi-active versus passive or active tuned mass dampers for structural control," *Journal of Engineering Mechanics*, vol. 109(9), pp. 691–705, 1983.

[48] N. R. Sandell, Jr., P. Varaiya, M. Athans, and M. G. Safonov, "Survey of decentralized control methods for large scale systems," *IEEE Transactions on Automatic Control*, vol. 23(2), pp. 108–128, 1978.

TABLE III

PERFORMANCE OBJECTIVES EVALUATED USING SCHEMES 1, 2, 3A, AND 3B FOR TWELVE CASES OF PULSE-PERIOD AND PULSE-VELOCITY. ITALICIZED VALUES ARE AT LEAST 10% BETTER THAN THE NEXT BEST CONTROL RESULT.

	Weak: $V_{\mathrm{p}x}, V_{\mathrm{p}y} = 0.5$ m/s, $V_{\mathrm{p}\theta} = 0.3$ rad/s						**Moderate**: $V_{\mathrm{p}x}, V_{\mathrm{p}y} = 1.0$ m/s, $V_{\mathrm{p}\theta} = 0.5$ rad/s						**Strong**: $V_{\mathrm{p}x}, V_{\mathrm{py}} = 1.2 m/s$, $V_{\mathrm{p}\theta} = 0.6$ rad/s					
	Short-period: $T_{\mathrm{p}} \ll T_{\mathrm{n}x}$						**Short-period:** $T_{\mathrm{p}} \ll T_{\mathrm{n}x}$						**Short-period:** $T_{\mathrm{p}} \ll T_{\mathrm{n}x}$					
Scheme	J $[10^6]$	Π_1	Π_2	Π_3	Π_4	Π_5	J $[10^6]$	Π_1	Π_2	Π_3	Π_4	Π_5	J $[10^6]$	Π_1	Π_2	Π_3	Π_4	Π_5
1	*0.09*	*0.34*	*0.21*	*0.41*	1.04	1.08	*0.36*	*0.69*	*0.21*	*0.45*	1.04	1.12	*0.52*	*0.82*	*0.21*	*0.44*	1.04	1.12
2	0.37	0.55	0.32	0.77	0.96	0.99	1.47	1.00	0.32	0.92	0.95	1.20	2.02	1.00	0.32	0.91	0.97	1.17
3a	1.87	1.00	0.70	1.16	0.90	1.05	4.47	1.00	0.50	2.56	1.10	2.94	5.60	1.00	0.48	2.67	1.17	3.27
3b	0.95	0.71	0.56	1.30	1.02	0.94	3.27	1.00	0.50	1.79	1.05	1.68	4.29	1.00	0.47	2.04	1.09	2.09
	Intermediate-period: $T_{\mathrm{p}} < T_{\mathrm{n}x}$						**Intermediate-period:** $T_{\mathrm{p}} < T_{\mathrm{n}x}$						**Intermediate-period:** $T_{\mathrm{p}} < T_{\mathrm{n}x}$					
1	*0.93*	1.00	0.74	1.96	1.14	1.01	*3.98*	1.00	0.77	2.09	1.18	*1.18*	*6.10*	1.00	0.81	2.13	1.24	*1.33*
2	1.36	0.80	0.76	1.72	1.07	1.12	5.61	1.00	0.81	*1.81*	1.09	1.70	8.37	1.00	0.86	*1.81*	1.17	1.97
3a	2.85	1.00	1.05	*1.15*	*0.68*	*0.80*	10.7	1.00	1.06	2.41	1.06	2.38	15.04	1.00	1.10	2.68	1.20	3.11
3b	2.54	0.81	1.05	1.32	0.98	1.18	9.91	1.00	1.11	2.35	1.16	2.24	14.14	1.00	1.13	2.56	1.26	2.77
	Resonant-period: $T_{\mathrm{p}} \approx T_{\mathrm{n}x}$						**Resonant-period:** $T_{\mathrm{p}} \approx T_{\mathrm{n}x}$						**Resonant-period:** $T_{\mathrm{p}} \approx T_{\mathrm{n}x}$					
1	2.12	0.60	1.20	1.40	0.44	0.58	8.56	1.00	1.26	1.42	0.46	0.76	13.08	1.00	1.35	1.60	0.50	*0.77*
2	3.34	0.75	1.66	3.19	0.89	1.33	14.01	1.00	1.68	3.60	0.90	1.37	22.05	1.00	1.72	3.60	0.92	2.04
3a	2.17	0.60	1.27	1.09	0.41	0.59	8.78	1.00	1.33	1.11	0.43	0.73	13.38	1.00	1.41	*1.11*	0.48	0.86
3b	2.82	0.51	1.49	1.13	0.60	0.80	11.25	1.00	1.50	1.16	0.60	0.96	16.66	1.00	1.54	1.16	0.62	0.98
	Long-period: $T_{\mathrm{p}} > T_{\mathrm{n}x}$						**Long-period:** $T_{\mathrm{p}} > T_{\mathrm{n}x}$						**Long-period:** $T_{\mathrm{p}} > T_{\mathrm{n}x}$					
1	1.39	0.40	1.30	1.27	0.24	0.39	5.53	0.80	1.31	1.25	0.25	0.47	7.96	0.96	1.31	1.25	0.25	0.47
2	2.10	0.53	1.78	2.61	0.45	1.12	8.37	1.00	1.79	2.86	0.45	1.23	12.10	1.00	1.78	2.98	0.45	1.32
3a	1.39	0.41	1.32	*1.14*	0.25	0.40	5.54	0.81	1.32	1.16	0.25	0.46	7.98	0.97	1.32	1.16	0.25	0.46
3b	1.58	0.33	1.48	1.20	0.32	0.49	6.30	0.66	1.49	1.21	0.32	0.56	9.07	*0.79*	1.49	1.21	0.32	0.56